AMERICAN SOCIETY FOR MICROBIOLOGY | Antimicrobial Agents and Chemotherapy®

Various Evolutionary Trajectories Lead to Loss of the Tobramycin-Potentiating Activity of the Quorum-Sensing Inhibitor Baicalin Hydrate in *Burkholderia cenocepacia* Biofilms

Andrea Sass,[a] Lisa Slachmuylders,[a] Heleen Van Acker,[a] Ian Vandenbussche,[a] Lisa Ostyn,[a] Mona Bové,[a] Aurélie Crabbé,[a] Laurent R. Chiarelli,[b] Silvia Buroni,[b] Filip Van Nieuwerburgh,[c] Emmanuel Abatih,[d] Tom Coenye[a]

[a]Laboratory of Pharmaceutical Microbiology, Ghent University, Ghent, Belgium
[b]Department of Biology and Biotechnology, University of Pavia, Pavia, Italy
[c]Laboratory of Pharmaceutical Biotechnology, Ghent University, Ghent, Belgium
[d]FIRE Unit, Department of Applied Mathematics, Computer Sciences and Statistics, Ghent University, Ghent, Belgium

ABSTRACT Combining antibiotics with potentiators that increase their activity is a promising strategy to tackle infections caused by antibiotic-resistant bacteria. As potentiators do not interfere with essential processes, it has been hypothesized that they are less likely to induce resistance. However, evidence supporting this hypothesis is lacking. In the present study, we investigated whether *Burkholderia cenocepacia* J2315 biofilms develop reduced susceptibility toward one such adjuvant, baicalin hydrate (BH). Biofilms were repeatedly and intermittently treated with tobramycin (TOB) alone or in combination with BH for 24 h. After treatment, the remaining cells were quantified using plate counting. After 15 cycles, biofilm cells were less susceptible to TOB and TOB+BH compared to the start population, and the potentiating effect of BH toward TOB was lost. Whole-genome sequencing was performed to probe which changes were involved in the reduced effect of BH, and mutations in 14 protein-coding genes were identified (including mutations in genes involved in central metabolism and in BCAL0296, encoding an ABC transporter). No changes in the MIC or MBC of TOB or changes in the number of persister cells were observed. However, basal intracellular levels of reactive oxygen species (ROS) and ROS levels found after treatment with TOB were markedly decreased in the evolved populations. In addition, in evolved cultures with mutations in BCAL0296, a significantly reduced uptake of TOB was observed. Our results indicate that *B. cenocepacia* J2315 biofilms rapidly lose susceptibility toward the antibiotic-potentiating activity of BH and point to changes in central metabolism, reduced ROS production, and reduced TOB uptake as mechanisms.

KEYWORDS *Burkholderia*, biofilms, evolution, quorum sensing, resistance

Due to increasing levels of antimicrobial resistance, novel strategies to tackle bacterial infections are needed, and an interesting approach is the use of antibiotic adjuvants or potentiators. Potentiators are compounds with little or no antibacterial activity that interfere with bacterial resistance mechanisms and/or increase antimicrobial activity when coadministered with an antibiotic (1–5). A well-known class of antibiotic adjuvants are quorum-sensing (QS) inhibitors (QSIs) (6). QSIs target the cell-density-based bacterial communication network that regulates the expression of multiple virulence factors (7, 8). Whether resistance would develop toward these adjuvants is currently unknown, and QSIs have long been accepted as "evolution-proof." Indeed, since QSIs do not target pathways essential for growth, it has been hypothesized that development of resistance would not occur (or at least would occur

Citation Sass A, Slachmuylders L, Van Acker H, Vandenbussche I, Ostyn L, Bové M, Crabbé A, Chiarelli LR, Buroni S, Van Nieuwerburgh F, Abatih E, Coenye T. 2019. Various evolutionary trajectories lead to loss of the tobramycin-potentiating activity of the quorum-sensing inhibitor baicalin hydrate in *Burkholderia cenocepacia* biofilms. Antimicrob Agents Chemother 63:e02092-18. https://doi.org/10.1128/AAC.02092-18.

Address correspondence to Tom Coenye, Tom.Coenye@UGent.be.

A.S. and L.S. contributed equally to this work.

Received 1 October 2018
Returned for modification 31 October 2018
Accepted 5 January 2019
Accepted manuscript posted online 22 January 2019
Published 27 March 2019

less frequently) due to the lack of selective pressure favoring the rise of resistant mutants (9–13). However, natural selection occurs when heritable variation provides a fitness advantage and QS disruption can affect bacterial fitness in conditions in which a functional QS system is essential (8). This was, for example, shown by cultivating *Pseudomonas aeruginosa* in medium with adenosine as a sole carbon source (14). As growth on adenosine depends on the production of a nucleoside hydrolase, which is positively regulated by the key QS signal receptor LasR, a functional QS system is required for the growth of *P. aeruginosa* under these conditions (15). After addition of the brominated furanone C-30 (a known QSI), growth of *P. aeruginosa* on adenosine was impaired, resulting in selective pressure and the occurrence of resistant mutants. Adding this QSI caused mutations in repressor genes of the multidrug resistance efflux pump MexAB-OrpM, which resulted in an increased resistance toward C-30 (14). Also in clinical *P. aeruginosa* isolates recovered from cystic fibrosis (CF) patients never exposed to C-30, mutations in these MexAB-OrpM repressor genes were found, leading to reduced susceptibility to C-30 (14, 16). Based on these results, Maeda et al. speculated that any strong selective pressure can induce resistance to antivirulence compounds (14, 17). In clinical practice, these adjuvants would be coadministered with an antibiotic. This means selective pressure imposed by this antibiotic needs to be included in the experimental setup when investigating possible development of resistance toward the adjuvants (1, 2). In addition, while most evolutionary studies on the development of resistance are carried out with planktonic cells (18–20), 65 to 80% of all infections are thought to be biofilm related, and biofilm-associated bacteria typically show a reduced susceptibility toward antimicrobial agents (21).

Burkholderia cenocepacia is an opportunistic pathogen that causes severe lung infections in people with CF, which can further develop into a life-threatening systemic infection known as the cepacia syndrome (22). Antimicrobial therapy in CF often fails due to the high innate resistance of *B. cenocepacia* toward many antibacterial agents and high tolerance associated with its biofilm lifestyle (22, 23). Previously, several adjuvants were identified that increased the activity of tobramycin (TOB) (an aminoglycoside antibiotic frequently used in CF lung infections) (24) toward *B. cenocepacia* biofilms, including the QSI baicalin hydrate (BH) (6, 25).

The goal of the present study is to evaluate whether (and how) *B. cenocepacia* J2315 biofilm cells can lose susceptibility toward the TOB-potentiating activity of BH. To this end, we used a slightly modified form of a previously described bead-based biofilm assay (26) in which *B. cenocepacia* J2315 cells were repeatedly and intermittently exposed to TOB, TOB+BH, or a control treatment (Fig. 1).

RESULTS AND DISCUSSION

Experimental evolution. Three lineages of *B. cenocepacia* J2315 cells were repeatedly and intermittently exposed to TOB (768 μg/ml, which equals three times the MIC), TOB (768 μg/ml) plus BH (250 μM) (TOB+BH), or a control treatment (Fig. 1). After 24 h of growth on the beads, Live/Dead staining was performed to evaluate biofilm formation (see Fig. S1 in the supplemental material). A dense biofilm was formed in the cavity of the doughnut-shaped bead (rather than on the exterior sides of the bead) with approximately 10^7 CFU/bead (prior to treatment).

The number of log(CFU/bead) after every cycle is shown in Fig. 2 and Table S1. After fitting a linear mixed-effect model (LMEM), using log(CFU/bead) as the dependent variable and cycle, treatment, lineage, and their two- and three-way interactions as fixed effects, and plotting the residuals against the corresponding fitted values, no departures from the main assumptions of normality and constancy of error variance were found. The remaining models were fit for each lineage separately following significance of the three-way interaction effect, and residuals were assessed for each of the models for each lineage. A detailed overview of the results of the statistical analysis can be found in Table S2.

The results indicated that for all lineages, the interaction effect between treatment and cycle was highly statistically significant ($P < 0.001$). A general observation within

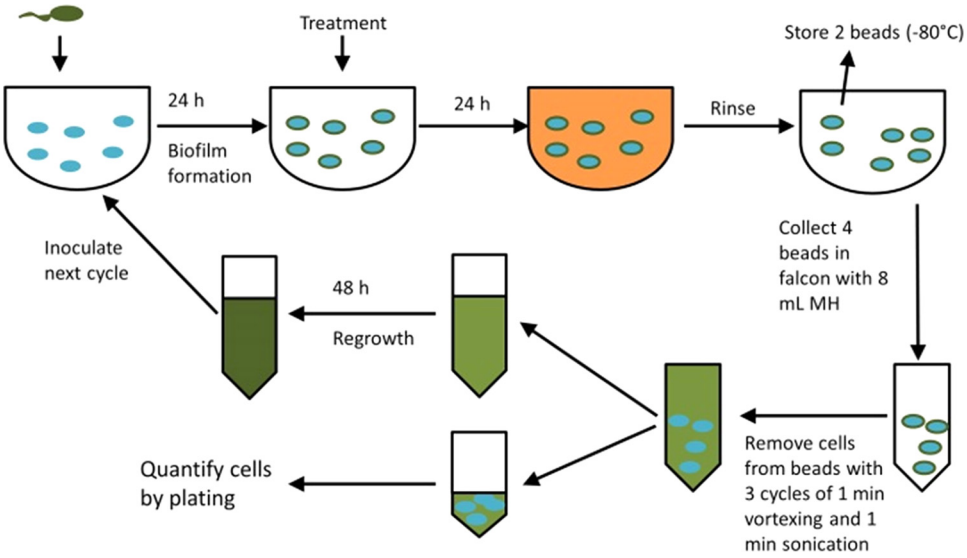

FIG 1 Experimental setup. Fresh inoculum is added to six cryobeads in the well of a 24-well microtiter plate. After 24 h, mature biofilms (gray circles) are formed on the surfaces of the beads. These biofilms are treated for 24 h. Afterward, the supernatant is removed, and the beads are rinsed with PS. Two beads, containing a mature biofilm, are stored at −80°C. The four other beads are transferred to a Falcon tube, in which the sessile cells from the beads are harvested. A part of these cells is used for quantification, while another part is used for planktonic regrowth of the cells (48 h).

each lineage was the significant difference in CFU recovered after TOB and the TOB+BH treatments compared to the control group (Table S2). The only exception was for lineage 2, wherein at cycle 11 this difference was not statistically significant ($P = 0.171$). Also, lineage 2 appeared to present more fluctuations in number of surviving cells, compared to lineages 1 and 3. At the start of the evolution experiment, the cells were significantly more susceptible to the TOB+BH combination than to TOB alone, confirming that BH potentiates the activity of TOB against biofilms, as previously shown (6, 27). Over time, biofilm-grown *B. cenocepacia* J2315 cells became gradually less susceptible to the treatment (both to treatment with TOB alone and to the TOB+BH combination treatment); this occurred in all three lineages (Fig. 2). The susceptibility to TOB+BH decreased faster than the susceptibility to TOB alone; differences in susceptibility between TOB+BH and TOB alone only persisted up to cycle 5, cycle 3, and cycle 4 for lineages 1, 2, and 3, respectively (Fig. S2 and Table S2).

Genome analysis. To investigate the reason behind this decreased susceptibility, whole-genome sequencing was performed. The results are summarized in Table 1. When considering all (nine) evolved lines, changes in 18 protein-coding genes were observed, as well as a partial deletion of two larger regions. Some changes were common and appeared in all evolved cultures at the same location (e.g., changes in BCAL1315, BCAL1664, and BCAM0949); we speculate that these mutations were already present in the starting population at low frequency and were enriched for during the experimental evolution. Other changes occurred only in one or a few samples (e.g., mutations in BCAL0929, BCAL2476a, and BCAM1901) and likely arose during the evolution study. For several genes that were mutated in multiple evolved cultures, we noticed the occurrence of different types of mutations (e.g., BCAL0269, BCAL1525, and BCAM0965).

All evolved cultures had mutations in the 5′ untranslated region (5′ UTR) of BCAL1525 (either a single nucleotide polymorphism (SNP) or insertion of a transposase at variable locations; Table 1). BCAL1525 encodes an Flp pilus assembly protein and has a 307-nucleotide and strongly expressed 5′ UTR with multiple transcription start sites (TSS) (28). BCAL1525 to BCAL1536 seem to form an operon with Flp pilus genes, although there is a terminator at positions 1690709 to 1690746 between BCAL1525 and

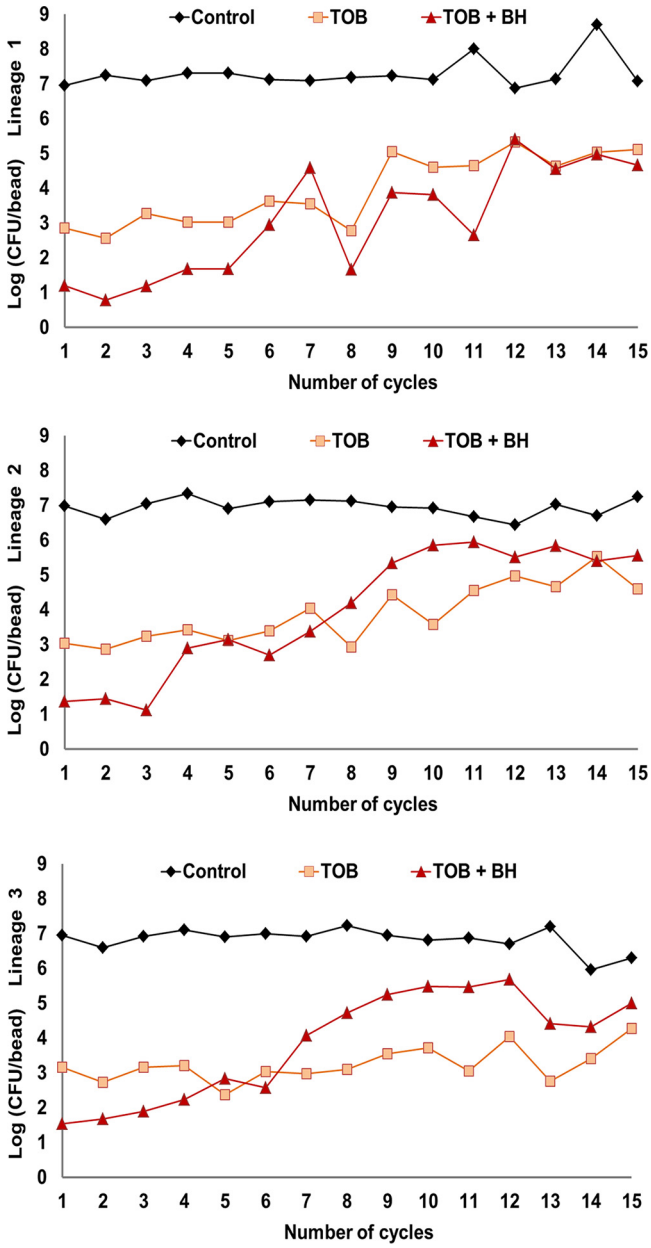

FIG 2 Numbers of *B. cenocepacia* J2315 biofilm cells, expressed as log(CFU/bead), in the untreated control (Control) and after repeated treatments with TOB or TOB+BH. (Top) Lineage 1; (middle) lineage 2; (bottom) lineage 3.

BCAL1526, and no further downstream TSS could be identified (28). Flp pili belong to the type IVb pilus family (29), which is poorly characterized in *Burkholderia* species. In *P. aeruginosa* type IV pili are thought to play a role in biofilm formation (30), although recent data suggest this may depend on the biofilm model system used (31). Mutations in BCAL1525 occur at high frequency in all evolved cultures, irrespective of the treatment, suggesting that there is an evolutionary pressure to lose the pilus function in the given experimental conditions. Since biofilm formation is not affected in the course of the experiment (Fig. 2), this indicates the Flp pilus is not required for biofilm formation under these conditions.

BCAL0296 encodes both the transmembrane and nucleotide binding domains of an ABC transport protein, and it is the only gene which is mutated in all treated evolved populations (except for one evolved population treated with TOB) but not in the

TABLE 1 Mutations observed in evolved populations

Gene	Function	Type	Variant/reference ratio (%)[a]									
			Start culture	Contr 1	Contr 2	Contr 3	TOB 1	TOB 2	TOB 3	TOB+BH 1	TOB+BH 2	TOB+BH 3
BCAL0296	ABC transporter component, peptide transporter	Deletion from BCAL0294 to BCAL0296 (328273 to 330830)					91					
BCAL0296	ABC transporter component, peptide transporter	Stop codon in CDS (330739 G to T, S331STOP)					100[a]	99		100	100	
BCAL0296	ABC transporter component, peptide transporter	SNP in CDS (330925 A to T, I269N)										100
BCAL0736	PTS system EI component, carbohydrate transport	Deletion in CDS, 18 bp, 2 different locations, both in frame			100	91			98			
BCAL0929	DeoR family glycerol-3-phosphate regulon repressor, GlpR	Deletion in CDS (10 bp 1012042 to 1012051)		100								
BCAL1172	Conserved hypothetical protein, in BcenGI5	Deletion of first 148 bp of gene		100								92
BCAL1315	Conserved hypothetical protein, in BcenGI6	Transposase inserted in CDS, same location	21	99	98	97	98	95	96	96	97	97
BCAL1525	Flp pilus assembly protein	SNP in 5′ UTR (1690247 G to C)			96							
BCAL1525	Flp pilus assembly protein	Transposase(s) inserted in 5′ UTR at various locations[c]		96		79	97	94	100	29	96	94
BCAL1664	Conserved hypothetical protein	SNP in 5′ UTR (1818909 G to A)	51	100	100	100	100	100	100	100	100	100
BCAL2476[b]	Conserved hypothetical protein fragment, in BcenGI8	Transposase inserted in 5′ UTR		97								
BCAL2628	Heme biosynthesis-associated TPR protein	Stop codon in CDS (2889248 C to A, E232STOP)			96	89			77			
BCAL2631	Phosphoenolpyruvate carboxylase	2 SNPs in CDS (2895340 to 2895341 GC to TT, R724C)									81	
BCAL3040	ABC-type sugar transport system, permease component	SNP in CDS (3332415 A to G, F51L)										100
BCAM0821	Methyl-accepting chemotaxis protein	SNP in CDS (907087 G to T, A369C)				52						
BCAM0949	Exported lipase LipA	SNP in CDS (1051105 C to G, S180W)	47	100	100	100	100	100	100	100	100	100
BCAM0965	Malate dehydrogenase	SNP in CDS (1070727 C to G, W254C)								58		
BCAM0965	Malate dehydrogenase	Stop codon in CDS (1070776 G to T, S238STOP)									100	
BCAM1204	Alanine racemase, catabolic	SNP in 5′ UTR (1316206 C to T)									100	
BCAM1870	CepI	SNP in CDS (2088576 C to G, C131W)						99		99	100	
BCAM1901	Hypothetical phage protein	Transposase inserted in CDS									93	
BCAM2284	Enolase	SNP in CDS (2566450 G to A, P103S)			100	99			99			
BCAL1017-BCAL1028	Includes diguanylate cyclase BCAL1020	Partial deletion of duplicated region[d]	20	100	100	100	100	100	100	100	100	100
BCAL2581-BCAL2591		Partial deletion of BcenGI8	50	100	100	100	100	100	100	100	100	100

[a]Numbers represent variant-to-reference ratios in percentages (calculated for each locus by dividing the number of mapped reads with sequence different from the reference genome by the number of mapped reads with sequence identical to the reference genome).

[b]The region is deleted in 91% of the population; the remaining 9% all have an SNP in this gene.

[c]Genome positions of transposase insertions into BCAL1525 5′ UTR are as follows. Contr 1, TOB+BH 2, and TOB+BH 3: 1690210; Contr 3: 1690218 and 1690239; TOB 1: 1690239; TOB 2: 1690196; TOB 3: 1690196, 1690206, 1690210, 1690218, and 1690239; and TOB+BH 1: 1690196 and 1690228. The orientation of the transposase is variable.

[d]The deleted genes are still present in the genome but are no longer duplicated.

control evolved populations; three different types of mutations are observed in this gene (a deletion, a nonsense mutation, and a nonsynonymous substitution; Table 1). In the lineage that does not have mutations in BCAL0296 (TOB 3), we observed several mutations that do not occur in other treated populations (i.e., in BCAL0736, BCAL2628, and BCAM2284), but the function of these genes does not allow us to link them to the reduced TOB susceptibility observed in biofilms of this lineage.

Three mutated genes are related to central metabolism and occur in TOB+BH-treated lineages only. BCAL2631 and BCAM0965 are both involved in oxaloacetate production. The mutation in BCAL2631 occurs only in one population exposed to TOB+BH; this gene encodes phosphoenol pyruvate kinase, which converts phosphoenol pyruvate to oxaloacetate in the "reverse tricarboxylic acid (TCA) cycle." Its activity typically results in increased oxaloacetate levels and an increased flux through the TCA cycle (32). It was designated as conditionally essential in *B. cenocepacia* J2315 in a minimal medium with only glucose as the substrate (33). BCAM0965 (encoding malate dehydrogenase) is mutated in two out of three evolved populations exposed to TOB+BH. Just like phosphoenol pyruvate kinase, malate dehydrogenase (which converts malate to oxaloacetate) activity will increase cellular oxaloacetate levels, likely stimulating the TCA cycle. BCAM0965 is also conditionally essential in *B. cenocepacia* J2315 (33). On top of that, in one TOB+BH-exposed evolved population, a mutation in a gene encoding the permease of a glucose/mannose ABC transporter (BCAL3040) was observed, likely affecting the uptake of certain carbohydrates.

None of the mutations observed were located in genes known to be responsible for aminoglycoside resistance, such as genes encoding aminoglycoside-modifying enzymes, efflux pumps, or ribosome methyltransferases, or in genes encoding ribosomal RNAs (34, 35). Since mutations in these genes often come at the cost of reduced relative growth fitness (36), the regrowth phase between treatment cycles might have prevented the accumulation of such mutations.

Role of QS and QSI. BH was previously described as a QSI (6), and in a recent study we showed it also has QS-independent activities, including modulating the oxidative stress response, that potentiate TOB in *B. cenocepacia* (27). To evaluate whether BH directly inhibits the *N*-octanoyl-L-homoserine lactone synthase CepI (37, 38), an enzymatic assay with purified CepI was carried out. CepI enzymatic activity was first tested at the concentration of BH slightly below that used for the evolution study (200 μM), and at this concentration BH completely inhibits CepI. Subsequently, the 50% inhibitory concentration (IC_{50}) was determined (46.8 $\pm$ 6.8 μM), which confirmed that BH inhibits CepI in a concentration-dependent way (Fig. S3). The mutation in BCAM1870, coding for CepI, is found in two evolved populations exposed to TOB+BH and in a single population exposed to TOB only; the same mutation (C131W) is found in these three populations. In order to investigate the effect of the C131W mutation, we introduced this mutation in wild-type CepI by site-directed mutagenesis and characterized the mutant enzyme. The enzyme was also inhibited by BH, showing a 2-fold-higher IC_{50} value (92.8 $\pm$ 4.5 μM). However, overall the kinetic properties were not significantly different from the wild-type enzyme (Fig. S3). This suggests that the Cys residue at position 131 is somehow involved in the binding of BH, despite its location in a region of the enzyme far from the binding site of other CepI inhibitors (39). Using qPCR, we investigated the expression of *cepI* (BCAM1870) and two QS-regulated genes (*aidA* [BCAS0293] and *zmpA* [BCAS0409]) (38) in cultures derived from the TOB-exposed biofilm of lineage 2. In stationary phase, the expression levels of these genes were not altered, but lower expression levels for these genes were observed in late log-phase cultures of the *cepI* mutant, with remarkably low levels of *aidA* expression (approximately 60-fold-lower expression compared to the control) (Fig. 3). This confirms that QS is indeed affected in this mutant. How the mutation in *cepI* contributes to an increased fitness of the evolved *B. cenocepacia* populations is currently unknown.

Phenotypic characterization of evolved lines. The lack of mutations in known TOB resistance genes suggested that the overall gradual decrease in susceptibility of *B.*

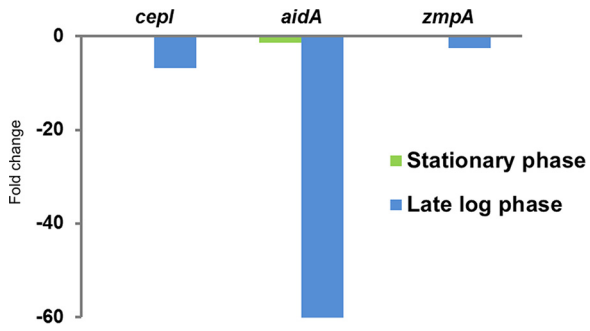

FIG 3 Expression of *cepI*, *aidA*, and *zmpA* in TOB-exposed evolved lineage compared to the control lineage, as determined by qPCR. Data shown are the fold change in the TOB-exposed lineage compared to the control. In late log phase, expression of *cepI* ($P < 0.05$) and *aidA* ($P < 0.01$) is significantly lower in the TOB-exposed lineage.

cenocepacia J2315 biofilm cells treated with TOB alone is not caused by a resistance mechanism specific for TOB. This is in line with the MIC and MBC values for TOB obtained for the different lineages (Table 2): in the presence or absence of BH, the MIC and MBC values for TOB in the evolved lines are equal to or within one 2-fold dilution of the values obtained for the start culture.

Second, we determined whether the evolutionary changes affected the number of persister cells in treated cultures (experiments concerning persisters were carried out in 2-fold with lineage 3 only). Persisters are known to occur in *B. cenocepacia* biofilms (40), and mutations leading to an increased fraction of persisters could (at least partially) explain the reduced effect of TOB+BH in the evolved lineages. However, the fraction of persisters recovered from *B. cenocepacia* J2315 biofilms after exposure to 4× MIC TOB were low and very similar for the control (0.0224%), the culture evolved in the presence of TOB (0.0393%), and the culture evolved in the presence of TOB+BH (0.0548%), ruling out increased persister formation as a source for the diminishing effect of TOB+BH (Fig. S4).

The evolved lines, including the untreated control, showed a marginally higher growth rate in the initial growth phases compared to untreated controls from cycle 1 (Fig. S5). All lines grew largely to the same final optical density, although the TOB+BH-treated lineage 2 always had the lowest optical density compared to the other lines

TABLE 2 MIC and MBC of TOB in *B. cenocepacia* J2315 recovered from different samples[a]

Sample	Treatment	MIC of TOB (μg/ml)	MBC of TOB (μg/ml)
Start culture	TOB	256	256
	TOB+BH	256	256
Lineage 1, treated with TOB	TOB	128	128
	TOB+BH	128	128
Lineage 1, treated with TOB+BH	TOB	256	256
	TOB+BH	128	256
Lineage 2, treated with TOB	TOB	128	128
	TOB+BH	128	128
Lineage 2, treated with TOB+BH	TOB	128	128
	TOB+BH	128	128
Lineage 3, treated with TOB	TOB	256	256
	TOB+BH	256	256
Lineage 3, treated with TOB+BH	TOB	256	512
	TOB+BH	512	512

[a]MIC and MBC were determined in presence (TOB+BH) or absence (TOB) of BH.

(Fig. S5). Interestingly, this is also the only lineage that has mutations in two conditionally essential genes (BCAL2631 and BCAM0965) (33), potentially explaining this growth phenotype. This suggests that the regrowth phase could be an evolutionary driving force, in addition to antibiotic treatment, and mutations leading to faster growth in initial phases would be expected to be present in all evolved lineages. This is indeed the case, e.g., mutations affecting the pilus assembly protein BCAL1525 possibly accelerate growth in the surrounding growth medium by allowing the cells to stay in the more oxygenated planktonic phase instead of attaching to the surface of the bead at the bottom of the wells. In addition, the partial deletions of genomic islands would decrease genome size and could increase the replication rate. However, the number of cells on the beads of untreated control lineages remained unchanged during the experiment, showing that these mutations did not affect biofilm formation. The regrowth phase is possibly responsible for the lack of mutations leading to tobramycin resistance and for the lack of mutations in antibiotic targets or mutations, which could lead to increased expression of canonical resistance genes, such as efflux pumps. Mutations that lead to increased resistance are generally associated with a decreased fitness of the mutant (36, 41, 42), and individual cells with such mutations would have been outcompeted during regrowth. However, the decreased growth of the TOB+BH-treated lineage 2 shows that growth characteristics were not the only evolutionary driving force in this experiment, and the nature of the mutations present only in treated lineages shows that treatment of the beads did have a specific impact.

Subsequently, we investigated whether there were differences in production of reactive oxygen species (ROS) between the start culture and the evolved populations. We have previously shown that bactericidal antibiotics (including TOB) induce ROS in *B. cenocepacia* biofilms and that this contributes to the antibiotic-mediated killing in *B. cenocepacia* (40, 43, 44). In addition, we have previously shown that BH increases TOB-induced oxidative stress in a QS-independent way (27). ROS are an inevitable by-product of aerobic respiration and, as we observed mutations in genes involved in oxaloacetate production (BCAL2631 and BCAM0695) or glucose/mannose transport (BCAL3040) in all lineages treated with TOB+BH (but not in lineages treated with TOB alone or in control lineages; Table 1), we hypothesized these mutations could affect ROS levels. First, we investigated if basal ROS levels (i.e., ROS levels observed in the absence of a treatment with a bactericidal antibiotic) were different between the start culture and the evolved populations. For the control populations and populations treated with TOB, significantly increased basal ROS levels were observed in two and one of the lineages, respectively (Fig. 4, top panel). For two of the populations that evolved in the presence of TOB+BH, a significant decrease in basal ROS production was observed ($P < 0.05$) (Fig. 4, top panel). These were also the populations in which mutations in BCAL2631 and/or BCAM0965 (thought to coregulate TCA activity) were observed. When ROS levels were determined after exposure to TOB, increased ROS production was observed for one of the control populations while no significant difference was observed for any of the populations evolved in the presence of TOB alone ($P < 0.05$) (Fig. 4, bottom panel). All populations evolved in the presence of TOB+BH showed reduced ROS levels compared to the start culture after treatment with TOB; this difference was significant ($P < 0.05$) for two lineages (Fig. 4, bottom panel).

Homologues of the putative ABC transporter BCAL0296, mutated in most evolved treated populations (but not in the controls), have been characterized in other bacteria. In *Bradyrhizobium* sp. the transporter homologue BclA is involved in protection against stress by antimicrobial peptides (45). BclA has multidrug transport activity and is involved in uptake of peptide-derived/peptide-like compounds, including bleomycin (46). The homologue in *Mycobacterium tuberculosis* is involved in uptake of vitamin B_{12} and bleomycin (47). It is therefore possible that BCAL0296 can import TOB into the cytoplasm under the experimental conditions used. To investigate this, we used a flow cytometry based assay to determine uptake of BODIPY-conjugated TOB. While there are no statistically significant differences when all nine groups (three lineages, three treatments) are compared (Fig. S6), differences in TOB uptake become apparent

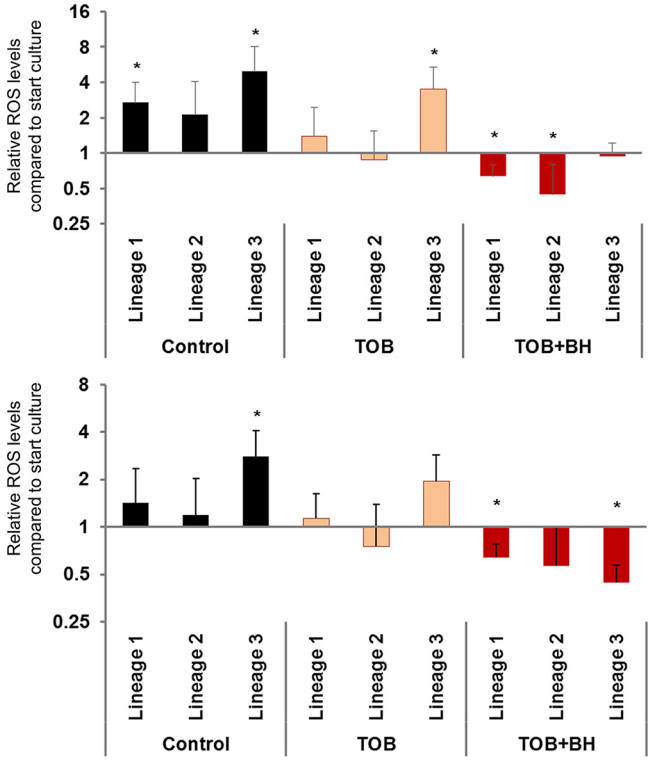

FIG 4 (Top) Basal ROS levels in evolved populations (relative compared to the start culture). (Bottom) ROS levels in evolved populations after exposure to 4× the MIC TOB (relative compared to start culture). The data shown are averages, and error bars represent standard errors ($n = 3 \times 5$). Statistically significant differences ($P < 0.05$) are indicated by an asterisk.

between treatments when data for the three treatments are averaged over the different lineages (Fig. 5), with TOB uptake significantly higher in the evolved control lines than in the evolved lines exposed to TOB ($P = 0.045$) or TOB+BH ($P < 0.001$). No significant difference was observed between the TOB and the TOB+BH exposed cultures. The results from this assay show that there is a significantly higher fraction of the population positive for BODIPY-TOB in evolved cultures without a mutation in BCAL0296 (i.e., the controls) than in evolved cultures with a mutation in BCAL0296 (i.e., the ones exposed to TOB or TOB+BH) (Fig. 5). These data suggest that BCAL0296 is involved in TOB import in *B. cenocepacia* and that the mutations occurring after repeated exposure to TOB or TOB+BH contribute to the reduced antimicrobial activity of TOB observed.

Conclusion. In the present study, we demonstrate that during experimental evolution *in vitro*, *B. cenocepacia* J2315 biofilms gradually become less susceptible to TOB and TOB+BH. Mutations in genes belonging to different functional categories were

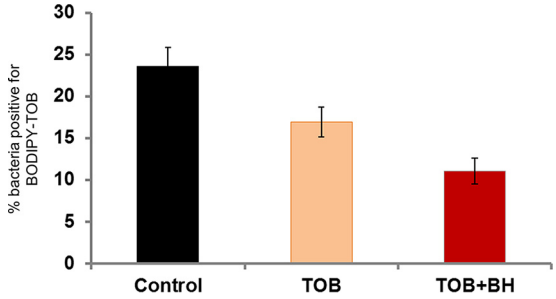

FIG 5 Differences in TOB uptake between treatments (based on averaged data over the different lineages). The data shown are averages, and error bars indicate standard errors ($n = 24$). TOB uptake is significantly lower in lineages exposed to TOB ($P = 0.045$) and TOB+BH ($P < 0.001$).

observed in the evolved populations exposed to the combination of TOB and BH, and some point to modifications in metabolism as a mechanism underlying the reduced susceptibility. The reduced levels of ROS (both basal levels and levels induced after exposure to TOB) observed in the lineages treated with TOB+BH point in the same direction. In addition, most lineages exposed to TOB or TOB+BH had mutations in BCAL0296, encoding an ABC transporter. Cells from populations in which BCAL0296 was mutated were more likely to accumulate lower levels of TOB intracellularly, providing an additional explanation for the reduced susceptibility of these evolved lineages. Although some genetic changes were found in multiple evolved populations, different lineages exposed to the same treatment appeared to have used different evolutionary trajectories to counteract the potentiating activity of BH. Our results indicate that loss of susceptibility to potentiators can develop in multiple ways, and this might limit their clinical applicability. Finally, our data demonstrate that experimental evolution combined with high-throughput sequencing can indeed identify the genetic changes behind reduced susceptibility and allows the identification of hitherto-unknown genes of interest likely involved in *B. cenocepacia* biofilm resistance and tolerance (48).

MATERIALS AND METHODS

Strains and culture conditions. *B. cenocepacia* J2315 (LMG 16656) was stored at −80°C using Microbank vials (Prolab Diagnostics, Richmond Hill, Ontario, Canada) and subcultured at 37°C on tryptone soy agar (TSA; Lab M, Lancashire, United Kingdom). Overnight cultures were grown aerobically in Mueller-Hinton broth (MHB; Lab M) at 37°C.

Reagents. Tobramycin (TOB; TCI Europe, Zwijndrecht, Belgium) was dissolved in physiological saline (PS; 0.9% [wt/vol] NaCl; Applichem, Darmstadt, Germany), filter sterilized (0.22 μm; Whatman, Dassel, Germany), and stored at 4°C until use. Stock solutions of BH (Sigma-Aldrich, Bornem, Belgium) were prepared in dimethyl sulfoxide (DMSO; Sigma-Aldrich) and diluted in PS prior to use.

Biofilm formation on beads. The set-up for biofilm formation was inspired by that reported by Traverse et al. (26). Cryobeads from Microbank vials (Prolab Diagnostics) were used as the substrates for biofilm formation. The beads were rinsed with PS prior to use to remove the cryopreservative present in the Microbank vials. This was achieved by adding 1 ml of PS, vortexing the vial, removing the PS, and repeating this three times. Six beads were then transferred to the wells of a 24-well microtiter plate (MTP; SPL Lifescience, South Korea), and 1 ml of a diluted overnight culture of *B. cenocepacia* J2315 (containing approximately 5×10^7 CFU per ml of MHB) was used as inoculum. The MTP was statically incubated at 37°C for 24 h. To evaluate the ability of *B. cenocepacia* J2315 cells to form mature biofilms on the beads, Live/Dead staining (Live/Dead BacLight bacterial viability kit; Thermo Fisher Scientific, Invitrogen, Carlsbad, CA) was performed after 24 h of biofilm formation. The biofilms on the beads were visualized using an EVOS FL Auto cell imaging system (Thermo Fisher Scientific, Waltham, MA; Syto9, λ_{ex} = 470/22 nm and λ_{em} = 510/42 nm; propidium iodide, λ_{ex} = 531/40 nm and λ_{em} = 593/40 nm).

Evolution experiment. To evaluate the influence of repeated treatments on biofilm susceptibility, cells were exposed to 15 cycles of biofilm formation (24 h), treatment (24 h), and planktonic regrowth (48 h) (Fig. 1). The planktonic regrowth step was included to generate a sufficiently high number of cells to set up a new biofilm for the next cycle. Biofilms were treated with PS (untreated control), TOB alone (at a concentration of 768 μg/ml, which equals 3× the MIC), and TOB in combination with BH (250 μM). The concentration of TOB and BH was selected based on preliminary experiments: the concentrations used in the present study lead to a significant reduction in cell numbers compared to the untreated control, but not complete eradication, so that regrowth in the following cycles can occur. Three independent experiments (designated as lineages) were set up for each condition, i.e., TOB (tobramycin), TOB+BH, and an untreated control. The three lineages were started from three different overnight start cultures. Biofilms were grown as described above, and after 24 h the beads were rinsed with PS and treated with TOB or a combination of TOB+BH. After 24 h of treatment at 37°C, the supernatant was removed, and the beads were rinsed with PS. Each well contained six beads: two beads were transferred to Eppendorf tubes containing 8% DMSO (Sigma-Aldrich) in MH for storage at −80°C, while the four remaining beads were transferred to a Falcon tube containing 8 ml of MH medium. Sessile cells were detached from the beads by three cycles of vortexing (1 min, Vortex-Genie 2; Scientific Industries, Inc., Bohemia, NY) and sonication (1 min; Branson 3510; Branson Ultrasonics Corp., Danbury, CT). Then, 6 ml of this bacterial suspension was transferred to another tube, followed by incubation for 48 h for regrowth, while shaking at 250 rpm at 37°C (KS 4000i control; IKA Works, Wilmington, NC). The remaining 2 ml was used to determine the number of surviving cells per bead (CFU/bead) by plating.

Determination of the MIC and MBC. To verify whether possible changes in susceptibility over time were due to increased resistance toward TOB, the MIC and MBC for TOB were determined for the start and end populations. MICs were determined according to the EUCAST broth microdilution assay using flat-bottom 96-well MTPs (SPL Lifescience) (49). The MIC was defined as the lowest concentration with a similar optical density as uninoculated growth medium. Absorbance was measured at 590 nm with a multilabel MTP reader (EnVision; Perkin-Elmer LAS, Waltham, MA). All MIC determinations were performed in duplicate. The MBC was determined by plating the suspension used for the MIC test, and the

MBC was the lowest concentration that did not allow recovery of colonies after 48 h of incubation at 37°C.

Determination of the number of persisters in tobramycin-exposed *B. cenocepacia* J2315 biofilms. To determine whether the evolutionary changes affected persistence, the number of persisters surviving TOB treatment was compared between biofilms formed by the start and evolved cultures. Biofilms were grown in 96-well microtiter plates as described previously (50) and exposed for 24 h to TOB in a concentration of 4× the MIC (1,024 μg/ml) (40). Briefly, an inoculum suspension containing 5×10^7 CFU/ml was added to the wells of a round bottomed 96-well microtiter plate. After 4 h of adhesion, the supernatant was removed, and the plates were rinsed with PS. Subsequently, 100 μl of fresh MHB was added, and the plates were further incubated at 37°C. After 24 h, the supernatant was removed and 120 μl of a TOB solution in PS or 120 μl of PS (i.e., control) was added. After 24 h, the cells were harvested by vortexing and sonication (2×5 min; Branson 3510) and quantified by plating on Luria-Bertani agar. Ten wells were included per strain, and the experiment was repeated twice ($n = 3$).

Measurement of ROS levels. To investigate whether there were differences in the production of ROS between the start culture and the evolved lineages, ROS were measured in treated and untreated start and evolved cultures. To measure ROS planktonic cultures were exposed to 2′,7′-dichlorodihydrofluorescein diacetate (H2DCFDA) in a final concentration of 10 μM in Luria-Bertani broth (43). After 45 min of incubation protected from light, the cells were washed with phosphate-buffered saline (PBS) and treated with TOB in a concentration of 4× the MIC or pH-matched PBS (i.e., the untreated control solution with the same pH as the antibiotic solution) for 24 h. Fluorescence (λ excitation = 485 nm, λ emission = 535 nm) was measured using an Envision plate reader. The autofluorescence of bacterial cells incubated without the probe and background fluorescence of the buffer solutions was measured and taken into account when calculating the net fluorescence. For the planktonic cultures, an overnight culture was diluted to an optical density of 0.1 (approximately 10^8 cells/ml). After an additional 24 h of growth in a shaking warm water bath, cell suspensions at an optical density of 1 (approximately 10^9 cells/ml) were transferred to falcon tubes and centrifuged for 9 min at a 3,634 relative centrifugal force. Cells were resuspended in fresh medium with or without dye to measure ROS. Five wells were included per condition and the experiment was repeated twice ($n = 3 \times 5$).

Genome sequencing and data analysis. After planktonic regrowth of the cells, DNA was extracted using a modified bead-beater protocol, adapted from Mahenthiralingam et al. (51). RNase-treated DNA was then quantified using the BioDrop μLITE (BioDrop, Cambridge, UK). Genomic DNA from the start culture and all evolved cultures obtained after 15 cycles were sequenced. Libraries were prepared using the NEBNext kit from Illumina and sequenced either on an Illumina Nextseq 500 or on a HiSeq 4000, generating 150-bp paired-end reads (Table S3). The experimental protocols and the raw sequencing data of all samples can be found in ArrayExpress under accession number E-MTAB-6236. Sequenced reads were quality trimmed (error probability limit, 0.05) and mapped to the *B. cenocepacia* J2315 reference genome (34) using CLC Genomics Workbench version 11.0.1. (Qiagen, Aarhus, Denmark) with a cutoff 80% for similarity and a 50% mapped read length. The mapping parameters were as follows: match score, 1; mismatch cost, 2; insertion and deletion cost, 3. More than 98.6% of reads mapped to the reference genome for all samples (Table S3). The unmapped reads were *de novo* assembled in CLC Genomics Workbench, but no contigs with a coverage >10% of the average coverage of the respective sample were found, and gene acquisition was therefore excluded. In CLC Genomics Workbench, the InDels and Structural Variants tool was used to detect insertions and deletions, with a *P* value threshold of 0.0001. The output was manually screened on mapping patterns of unaligned read ends, and only entries with a single breakpoint and identical sequences in the unaligned read ends were reported. The consensus sequence of the unaligned read ends was then used to confirm the deletion or to identify the nature of the inserted sequence. A larger insertion sequence cannot be fully deduced in this manner, but only a certain type of transposase which was already present multiple times in the *B. cenocepacia* J2315 reference genome was detected: *Burkholderia cepacia* insertion element IS*407*. Both consensus sequences at insertion breakpoints were consistent with either end of this transposase, it was therefore concluded that the insertion consisted of only that transposase. The Basic Variant Detection tool was used to detect SNPs with a minimum coverage of 10 and a reference-to-variant ratio of 35%. This was the lowest cutoff that allowed us to clearly distinguish true SNPs from sequencing errors. All SNPs were then manually screened for false positives in regions containing repetitive sequences or hairpins, which caused poor mapping. The function of the genes that acquired mutational changes was determined using the Conserved Domain database (52) and *Burkholderia* Genome Database (53).

qPCR. Cultures from cycle 15, control lineage 3, and Tob lineage 2 were cultivated in MHB in a shaking incubator at 150 rpm for 6 to 10 h. Late-log-phase cultures were harvested at a density of 1×10^9 to 1.3×10^9 CFU/ml, and stationary-phase cultures were harvested at a density of 3×10^9 to 4.5×10^9 CFU/ml. Cell pellets were frozen at −80°C, and RNA was extracted within 1 week of harvest using a RiboPure bacteria kit (Thermo Fisher, Rochester, NY) according to the standard protocol, including DNase treatment. RNA was quantified with the BioDrop μLITE. cDNA was generated with a high-capacity cDNA reverse transcription kit (Applied Biosystems, Foster City, CA) from 500 ng of RNA. qPCR was performed in a CFX96 Real-Time System C1000 thermal cycler (Bio-Rad, Hercules, CA) using GoTaq qPCR Master Mix (Promega, Madison, WI). Cq values were normalized against a previously validated control gene (*rpoD*, BCAM0918) (54, 55). Fold changes were calculated compared to a standard (mix of all cDNAs in experiment) and log transformed. The primers are listed in Table S4.

Growth curves. Growth curves were determined in MHB. Portions (200 μl/well) of a 5×10^5 CFU/ml inoculum were added in triplicates to round-bottom MTPs, and the absorbance at 590 nm was measured

in a microplate reader (Envision; Perkin-Elmer, Shelton, CT), every 30 min for 50 h. The experiment was repeated three times, and representative curves are shown.

Determination of CepI activity in the presence of BH. *B. cenocepacia* CepI was expressed in *Escherichia coli* BL21(DE3) cells and purified according to a previously described procedure (56). The enzymatic activity was determined by a spectrophotometric assay according to Christensen et al. (57), which measures the *holo*-ACP formation by titrating the release of the free thiol of ACP with dichlorophenylindophenol (DCPIP; $\varepsilon = 19{,}100\ M^{-1}\,cm^{-1}$). Measurements were performed at 37°C, in a final volume of 100 μl, using an Eppendorf Biospectrometer. The standard reaction mixture contained 50 mM HEPES (pH 7.5), 0.005% Nonidet P-40, 0.13 mM DCPIP, 70 μM octanoyl-ACP (C8-ACP) (58, 59), and 4 μM CepI; the reactions were started by the addition of 40 μM *S*-adenosylmethionine (SAM) after preincubation for 10 min. CepI inhibition was initially screened at 200 μM BH (dissolved in DMSO). CepI inhibition was initially screened at 200 μM (dissolved in DMSO), and the IC_{50} was then determined by measuring the enzyme activities in the presence of different BH concentrations, and fitting data according to equation 1:

$$A_{[I]} = A_{[0]} \times \left(10\frac{[I]}{[I] + IC_{50}}\right) \quad (1)$$

where $A_{[I]}$ is the enzyme activity at BH concentration [*I*] and $A_{[0]}$ is the enzyme activity without BH. All measurements were performed in triplicate.

Site-directed mutagenesis of *cepI*. Plasmid pETSUMO-CepI (56) was used as the template for PCR mutagenesis experiment to generate the amino acid substitution C131W, using the primers CepC131Wfor (5′-GGCCGTCGTCGAATGGGCGGCCCAGCTCGGG-3′) and CepC131Wrev (5′-CCCGAGCTGG GCCGCCCATTCGACGACGGCC-3′). The site-directed mutagenesis was carried out as previously described (60) using HotStar HiFidelity Polymerase (Qiagen) and FastDigest DpnI (Thermo Fisher Scientific). The mutated CepIC131W was expressed and purified as described above for the wild-type protein.

Quantification of intracellular tobramycin levels. BODIPY-labeled tobramycin was synthesized as previously described (61). Bacteria were grown under biofilm-forming conditions for 4 h in MHB in the presence of 0.75 μg/ml BODIPY-tobramycin at 37°C. After 4 h of biofilm formation, the biofilm was rinsed to remove extracellular tobramycin, homogenized and subjected to flow cytometry analysis (Attune NxT; Life Technologies). The bacterial population was delineated based on the forward and side scatter signals, and a threshold was set to exclude noncellular particles and cell debris. BODIPY-tobramycin that associated with bacterial cells was determined through excitation with a 488-nm laser. Fluorescence emission was detected through a 530/30 bandpass filter. Controls included bacterial biofilm cells that were not exposed to BODIPY-tobramycin (negative control) or to incremental levels of tobramycin to determine the concentration at which saturation was obtained. Based on the negative control and the concentration of tobramycin where maximal population saturation was obtained, negative and positive flow cytometry gates, respectively, were determined. At least 10,000 bacteria were analyzed per sample.

Statistical analysis. To determine whether the observed variations in survival over time for the different treatments were statistically significant, a linear mixed-effect model (LMEM) was used. The model uses the log(CFU/bead) as the dependent variable and cycle, treatment, lineage, and their two- and three-way interactions as fixed effects and was fit using SAS version 9.4 (SAS Institute, Cary, NC). To account for possible correlations between the measurements over cycles, a compound symmetry variance covariance structure was used. All interaction effects that were not significant were excluded from the model. When an interaction was significant, this was considered the fixed effect to evaluate differences in treatment effect. Per lineage, treatments were compared pairwise to TOB treatment using the Tukey adjustment method. Assumptions associated with the LMEM were checked based on residuals from the fitted final model (Table S2).

Other data sets were analyzed using SPSS version 25 software (SPSS, Chicago, IL). The Shapiro-Wilk test was used to verify the normal distribution assumption of the data. Differences between the means of normally and not-normally distributed data were assessed using one-way analysis of variance testing or a Kruskal-Wallis nonparametric test, respectively, followed by a Dunnett's *post hoc* analysis. P values smaller than 0.05 were considered statistically significant.

SUPPLEMENTAL MATERIAL

Supplemental material for this article may be found at https://doi.org/10.1128/AAC.02092-18.

SUPPLEMENTAL FILE 1, PDF file, 0.8 MB.

ACKNOWLEDGMENTS

This study was supported by the Special Research Fund of Ghent University (grant BOF13/24j/017); the Belgian Science Policy Office (grant P7/28 of the Interuniversity Attraction Pole program); the Fund for Scientific Research (postdoctoral fellowship to HVA and Odysseus fellowship to A.C.); and the Italian Ministry of Education, University and Research (MIUR; Dipartimenti di Eccellenza Program 2018–2022, Department of Biology and Biotechnology L. Spallanzani, University of Pavia) (to L.R.C. and S.B.). The funders had no role in study design, data collection and interpretation, or the decision to submit the work for publication.

REFERENCES

1. Gill EE, Franco OL, Hancock RE. 2015. Antibiotic adjuvants: diverse strategies for controlling drug-resistant pathogens. Chem Biol Drug Des 85:56–78. https://doi.org/10.1111/cbdd.12478.
2. Bernal P, Molina-Santiago C, Daddaoua A, Llamas MA. 2013. Antibiotic adjuvants: identification and clinical use. Microb Biotechnol 6:445–449. https://doi.org/10.1111/1751-7915.12044.
3. Brown D. 2015. Antibiotic resistance breakers: can repurposed drugs fill the antibiotic discovery void? Nat Rev Drug Discov 14:821–832. https://doi.org/10.1038/nrd4675.
4. Brown ED, Wright GD. 2016. Antibacterial drug discovery in the resistance era. Nature 529:336–343. https://doi.org/10.1038/nature17042.
5. Wright GD. 2016. Antibiotic adjuvants: rescuing antibiotics from resistance. Trends Microbiol 24:862–871. https://doi.org/10.1016/j.tim.2016.06.009.
6. Brackman G, Cos P, Maes L, Nelis HJ, Coenye T. 2011. Quorum sensing inhibitors increase the susceptibility of bacterial biofilms to antibiotics *in vitro* and *in vivo*. Antimicrob Agents Chemother 55:2655–2661. https://doi.org/10.1128/AAC.00045-11.
7. Waters CM, Bassler BL. 2005. Quorum sensing: cell-to-cell communication in bacteria. Annu Rev Cell Dev Biol 21:319–346. https://doi.org/10.1146/annurev.cellbio.21.012704.131001.
8. Defoirdt T, Boon N, Bossier P. 2010. Can bacteria evolve resistance to quorum sensing disruption? PLoS Pathog 6:e1000989. https://doi.org/10.1371/journal.ppat.1000989.
9. Melander RJ, Melander C. 2017. The challenge of overcoming antibiotic resistance: an adjuvant approach? ACS Infect Dis 3:559–563. https://doi.org/10.1021/acsinfecdis.7b00071.
10. Hirakawa H, Tomita H. 2013. Interference of bacterial cell-to-cell communication: a new concept of antimicrobial chemotherapy breaks antibiotic resistance. Front Microbiol 4:114. https://doi.org/10.3389/fmicb.2013.00114.
11. Hentzer M, Wu H, Andersen JB, Riedel K, Rasmussen TB, Bagge N, Kumar N, Schembri MA, Song Z, Kristoffersen P, Manefield M, Costerton JW, Molin S, Eberl L, Steinberg P, Kjelleberg S, Hoiby N, Givskov M. 2003. Attenuation of *Pseudomonas aeruginosa* virulence by quorum sensing inhibitors. EMBO J 22:3803–3815. https://doi.org/10.1093/emboj/cdg366.
12. Gerdt JP, Blackwell HE. 2014. Competition studies confirm two major barriers that can preclude the spread of resistance to quorum-sensing inhibitors in bacteria. ACS Chem Biol 9:2291–2299. https://doi.org/10.1021/cb5004288.
13. Mellbye B, Schuster M. 2011. The sociomicrobiology of antivirulence drug resistance: a proof of concept. mBio 2:e00131-11.
14. Maeda T, García-Contreras R, Pu M, Sheng L, Garcia LR, Tomás M, Wood TK. 2012. Quorum quenching quandary: resistance to antivirulence compounds. ISME J 6:493–501. https://doi.org/10.1038/ismej.2011.122.
15. Heurlier K, Denervaud V, Haenni M, Guy L, Krishnapillai V, Haas D. 2005. Quorum-sensing-negative (lasR) mutants of *Pseudomonas aeruginosa* avoid cell lysis and death. J Bacteriol 187:4875–4883. https://doi.org/10.1128/JB.187.14.4875-4883.2005.
16. Tomas M, Doumith M, Warner M, Turton JF, Beceiro A, Bou G, Livermore DM, Woodford N. 2010. Efflux pumps, OprD porin, AmpC beta-lactamase, and multiresistance in *Pseudomonas aeruginosa* isolates from cystic fibrosis patients. Antimicrob Agents Chemother 54:2219–2224. https://doi.org/10.1128/AAC.00816-09.
17. Garcia-Contreras R, Maeda T, Wood TK. 2016. Can resistance against quorum-sensing interference be selected? ISME J 10:4–10. https://doi.org/10.1038/ismej.2015.84.
18. Steenackers HP, Parijs I, Dubey A, Foster KR, Vanderleyden J. 2016. Experimental evolution in biofilm populations. FEMS Microbiol Rev 40:373–397. https://doi.org/10.1093/femsre/fuw002.
19. Van den Bergh B, Swings T, Fauvart M, Michiels J. 2018. Experimental design, population dynamics, and diversity in microbial experimental evolution. Microbiol Mol Biol Rev 82. https://doi.org/10.1128/MMBR.00008-18.
20. Zhang Q, Lambert G, Liao D, Kim H, Robin K, Tung CK, Pourmand N, Austin RH. 2011. Acceleration of emergence of bacterial antibiotic resistance in connected microenvironments. Science (New York, NY) 333:1764–1767. https://doi.org/10.1126/science.1208747.
21. Van Acker H, Van Dijck P, Coenye T. 2014. Molecular mechanisms of antimicrobial tolerance and resistance in bacterial and fungal biofilms. Trends Microbiol 22:326–333. https://doi.org/10.1016/j.tim.2014.02.001.
22. Mahenthiralingam E, Urban TA, Goldberg JB. 2005. The multifarious, multireplicon *Burkholderia cepacia* complex. Nat Rev Microbiol 3:144–156. https://doi.org/10.1038/nrmicro1085.
23. Coenye T. 2010. Social interactions in the *Burkholderia cepacia* complex: biofilms and quorum sensing. Future Microbiol 5:1087–1099. https://doi.org/10.2217/fmb.10.68.
24. Scoffone VC, Chiarelli LR, Trespidi G, Mentasti M, Riccardi G, Buroni S. 2017. *Burkholderia cenocepacia* infections in cystic fibrosis patients: drug resistance and therapeutic approaches. Front Microbiol 8:1592. https://doi.org/10.3389/fmicb.2017.01592.
25. Luo J, Dong B, Wang K, Cai S, Liu T, Cheng X, Lei D, Chen Y, Li Y, Kong J, Chen Y. 2017. Baicalin inhibits biofilm formation, attenuates the quorum sensing-controlled virulence and enhances *Pseudomonas aeruginosa* clearance in a mouse peritoneal implant infection model. PLoS One 12:e0176883. https://doi.org/10.1371/journal.pone.0176883.
26. Traverse CC, Mayo-Smith LM, Poltak SR, Cooper VS. 2013. Tangled bank of experimentally evolved *Burkholderia* biofilms reflects selection during chronic infections. Proc Natl Acad Sci U S A 110:E250–E259. https://doi.org/10.1073/pnas.1207025110.
27. Slachmuylders L, Van Acker H, Brackman G, Sass A, Van Nieuwerburgh F, Coenye T. 2018. Elucidation of the mechanism behind the potentiating activity of baicalin against *Burkholderia cenocepacia* biofilms. PLoS One 13:e0190533. https://doi.org/10.1371/journal.pone.0190533.
28. Sass AM, Van Acker H, Forstner KU, Van Nieuwerburgh F, Deforce D, Vogel J, Coenye T. 2015. Genome-wide transcription start site profiling in biofilm-grown *Burkholderia cenocepacia* J2315. BMC Genomics 16:775. https://doi.org/10.1186/s12864-015-1993-3.
29. Roux N, Spagnolo J, de Bentzmann S. 2012. Neglected but amazingly diverse type IVb pili. Res Microbiol 163:659–673. https://doi.org/10.1016/j.resmic.2012.10.015.
30. Klausen M, Heydorn A, Ragas P, Lambertsen L, Aaes-Jorgensen A, Molin S, Tolker-Nielsen T. 2003. Biofilm formation by *Pseudomonas aeruginosa* wild type, flagella and type IV pili mutants. Mol Microbiol 48:1511–1524. https://doi.org/10.1046/j.1365-2958.2003.03525.x.
31. Davies EV, James CE, Brockhurst MA, Winstanley C. 2017. Evolutionary diversification of *Pseudomonas aeruginosa* in an artificial sputum model. BMC Microbiol 17:3. https://doi.org/10.1186/s12866-016-0916-z.
32. Sauer U, Eikmanns BJ. 2005. The PEP-pyruvate-oxaloacetate node as the switch point for carbon flux distribution in bacteria. FEMS Microbiol Rev 29:765–794. https://doi.org/10.1016/j.femsre.2004.11.002.
33. Wong YC, Abd El Ghany M, Naeem R, Lee KW, Tan YC, Pain A, Nathan S. 2016. Candidate essential genes in *Burkholderia cenocepacia* J2315 identified by genome-wide TraDIS. Front Microbiol 7:1288. https://doi.org/10.3389/fmicb.2016.01288.
34. Holden MT, Seth-Smith HM, Crossman LC, Sebaihia M, Bentley SD, Cerdeno-Tarraga AM, Thomson NR, Bason N, Quail MA, Sharp S, Cherevach I, Churcher C, Goodhead I, Hauser H, Holroyd N, Mungall K, Scott P, Walker D, White B, Rose H, Iversen P, Mil-Homens D, Rocha EP, Fialho AM, Baldwin A, Dowson C, Barrell BG, Govan JR, Vandamme P, Hart CA, Mahenthiralingam E, Parkhill J. 2009. The genome of *Burkholderia cenocepacia* J2315, an epidemic pathogen of cystic fibrosis patients. J Bacteriol 191:261–277. https://doi.org/10.1128/JB.01230-08.
35. Garneau-Tsodikova S, Labby KJ. 2016. Mechanisms of resistance to aminoglycoside antibiotics: overview and perspectives. MedChemComm 7:11–27. https://doi.org/10.1039/C5MD00344J.
36. Hughes D, Andersson DI. 2017. Evolutionary trajectories to antibiotic resistance. Annu Rev Microbiol 71:579–596. https://doi.org/10.1146/annurev-micro-090816-093813.
37. Sokol PA, Sajjan U, Visser MB, Gingues S, Forstner J, Kooi C. 2003. The CepIR quorum-sensing system contributes to the virulence of *Burkholderia cenocepacia* respiratory infections. Microbiology (Reading, England) 149:3649–3658. https://doi.org/10.1099/mic.0.26540-0.
38. Subsin B, Chambers CE, Visser MB, Sokol PA. 2007. Identification of genes regulated by the cepIR quorum-sensing system in *Burkholderia cenocepacia* by high-throughput screening of a random promoter library. J Bacteriol 189:968–979. https://doi.org/10.1128/JB.01201-06.
39. Buroni S, Scoffone VC, Fumagalli M, Makarov V, Cagnone M, Trespidi G, De Rossi E, Forneris F, Riccardi G, Chiarelli LR. 2018. Investigating the mechanism of action of diketopiperazines inhibitors of the *Burkholderia cenocepacia* quorum sensing synthase CepI: a site-directed mutagenesis study. Front Pharmacol 9:836. https://doi.org/10.3389/fphar.2018.00836.

40. Van Acker H, Sass A, Bazzini S, De Roy K, Udine C, Messiaen T, Riccardi G, Boon N, Nelis HJ, Mahenthiralingam E, Coenye T. 2013. Biofilm-grown *Burkholderia cepacia* complex cells survive antibiotic treatment by avoiding production of reactive oxygen species. PLoS One 8:e58943. https://doi.org/10.1371/journal.pone.0058943.
41. Andersson DI, Hughes D. 2010. Antibiotic resistance and its cost: is it possible to reverse resistance? Nat Rev Microbiol 8:260–271. https://doi.org/10.1038/nrmicro2319.
42. Durao P, Balbontin R, Gordo I. 2018. Evolutionary mechanisms shaping the maintenance of antibiotic resistance. Trends Microbiol 26:677–691. https://doi.org/10.1016/j.tim.2018.01.005.
43. Van Acker H, Gielis J, Acke M, Cools F, Cos P, Coenye T. 2016. The role of reactive oxygen species in antibiotic-induced cell death in *Burkholderia cepacia* complex bacteria. PLoS One 11:e0159837. https://doi.org/10.1371/journal.pone.0159837.
44. Van Acker H, Coenye T. 2017. The role of reactive oxygen species in antibiotic-mediated killing of bacteria. Trends Microbiol 25:456–466. https://doi.org/10.1016/j.tim.2016.12.008.
45. Barriere Q, Guefrachi I, Gully D, Lamouche F, Pierre O, Fardoux J, Chaintreuil C, Alunni B, Timchenko T, Giraud E, Mergaert P. 2017. Integrated roles of BclA and DD-carboxypeptidase 1 in *Bradyrhizobium* differentiation within NCR-producing and NCR-lacking root nodules. Sci Rep 7:9063. https://doi.org/10.1038/s41598-017-08830-0.
46. Guefrachi I, Pierre O, Timchenko T, Alunni B, Barriere Q, Czernic P, Villaecija-Aguilar JA, Verly C, Bourge M, Fardoux J, Mars M, Kondorosi E, Giraud E, Mergaert P. 2015. *Bradyrhizobium* BclA is a peptide transporter required for bacterial differentiation in symbiosis with *Aeschynomene* legumes. Mol Plant Microbe Interact 28:1155–1166. https://doi.org/10.1094/MPMI-04-15-0094-R.
47. Gopinath K, Venclovas C, Ioerger TR, Sacchettini JC, McKinney JD, Mizrahi V, Warner DF. 2013. A vitamin B_{12} transporter in *Mycobacterium tuberculosis*. Open Biol 3:120175. https://doi.org/10.1098/rsob.120175.
48. Cooper VS. 2018. Experimental evolution as a high-throughput screen for genetic adaptations. mSphere 3:e00121-18. https://doi.org/10.1128/mSphere.00121-18.
49. ESCMID. 2003. Determination of minimum inhibitory concentrations (MICs) of antibacterial agents by broth dilution. Clin Microbiol Infect 9:ix–xv. https://doi.org/10.1046/j.1469-0691.2003.00790.x.
50. Van Acker H, Van Snick E, Nelis HJ, Coenye T. 2010. *In vitro* activity of temocillin against planktonic and sessile *Burkholderia cepacia* complex bacteria. J Cystic Fibrosis 9:450–454. https://doi.org/10.1016/j.jcf.2010.08.015.
51. Mahenthiralingam E, Campbell ME, Foster J, Lam JS, Speert DP. 1996. Random amplified polymorphic DNA typing of *Pseudomonas aeruginosa* isolates recovered from patients with cystic fibrosis. J Clin Microbiol 34:1129–1135.
52. Marchler-Bauer A, Bo Y, Han L, He J, Lanczycki CJ, Lu S, Chitsaz F, Derbyshire MK, Geer RC, Gonzales NR, Gwadz M, Hurwitz DI, Lu F, Marchler GH, Song JS, Thanki N, Wang Z, Yamashita RA, Zhang D, Zheng C, Geer LY, Bryant SH. 2017. CDD/SPARCLE: functional classification of proteins via subfamily domain architectures. Nucleic Acids Res 45:D200–D203. https://doi.org/10.1093/nar/gkw1129.
53. Winsor GL, Khaira B, Van Rossum T, Lo R, Whiteside MD, Brinkman FS. 2008. The Burkholderia Genome Database: facilitating flexible queries and comparative analyses. Bioinformatics (Oxford, England) 24:2803–2804. https://doi.org/10.1093/bioinformatics/btn524.
54. Sass AM, Schmerk C, Agnoli K, Norville PJ, Eberl L, Valvano MA, Mahenthiralingam E. 2013. The unexpected discovery of a novel low-oxygen-activated locus for the anoxic persistence of *Burkholderia cenocepacia*. ISME J 7:1568–1581. https://doi.org/10.1038/ismej.2013.36.
55. Kiekens S, Sass A, Van Nieuwerburgh F, Deforce D, Coenye T. 2018. The small RNA ncS35 regulates growth in *Burkholderia cenocepacia* J2315. mSphere 3:e00579-17. https://doi.org/10.1128/mSphere.00579-17.
56. Scoffone VC, Chiarelli LR, Makarov V, Brackman G, Israyilova A, Azzalin A, Forneris F, Riabova O, Savina S, Coenye T, Riccardi G, Buroni S. 2016. Discovery of new diketopiperazines inhibiting *Burkholderia cenocepacia* quorum sensing *in vitro* and *in vivo*. Sci Rep 6:32487. https://doi.org/10.1038/srep32487.
57. Christensen QH, Grove TL, Booker SJ, Greenberg EP. 2013. A high-throughput screen for quorum-sensing inhibitors that target acylhomoserine lactone synthases. Proc Natl Acad Sci U S A 110:13815–13820. https://doi.org/10.1073/pnas.1313098110.
58. Cronan JE, Thomas J. 2009. Bacterial fatty acid synthesis and its relationships with polyketide synthetic pathways. Methods Enzymol 459:395–433. https://doi.org/10.1016/S0076-6879(09)04617-5.
59. Quadri LE, Weinreb PH, Lei M, Nakano MM, Zuber P, Walsh CT. 1998. Characterization of Sfp, a *Bacillus subtilis* phosphopantetheinyl transferase for peptidyl carrier protein domains in peptide synthetases. Biochemistry 37:1585–1595. https://doi.org/10.1021/bi9719861.
60. Bachman J. 2013. Site-directed mutagenesis. Methods Enzymol 529:241–248. https://doi.org/10.1016/B978-0-12-418687-3.00019-7.
61. Messiaen AS. 2013. Towards improvement of antibiotic therapy for treating Burkholderia cepacia complex biofilm infections in cystic fibrosis patients. PhD thesis. Ghent University, Gent, Belgium.